ChemComm

Accepted Manuscript

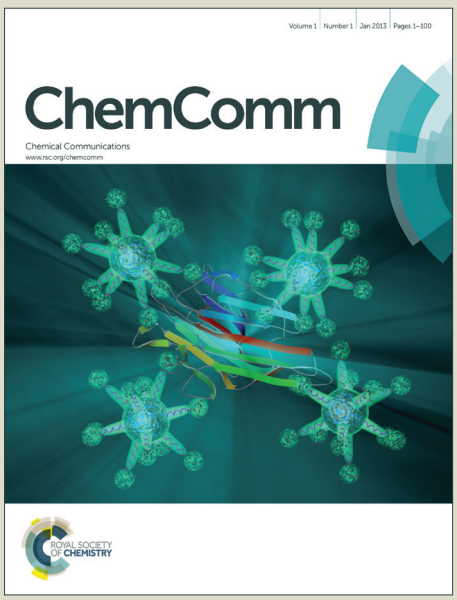

ROYAL SOCIETY OF CHEMISTRY

www.rsc.org/chemcomm

Journal Name RSCPublishing

COMMUNICATION

Monocrystalline mesoporous metal oxide with perovskite structure: a facile solid-state transformation of coordination polymer†

Cite this: DOI: 10.1039/x0xx00000x

Received 00th January 2012, Accepted 00th January 2012

DOI: 10.1039/x0xx00000x

www.rsc.org/

Li Xu [a†], Fan-Xing Bu [a†], Ming Hu *[a], Chuan-Yin Jin [a], Dong-Mei Jiang [a], Zhen-Jie Zhao [a], Qing-Hong Zhang [b], and Ji-Sen Jiang *[a]

Monocrystalline mesoporous $BiFeO_3$ crystals were obtained *via* a multi-step single-crystalline to single-crystalline transformation of a coordination polymer, $Bi[Fe(CN)_6]\cdot 4H_2O$. The unique transformation process significantly decreased the crystallization temperature of perovskite oxide without losing high crystallinity.

Mesoporous ceramics with crystalline framework exhibit great potential in high efficient catalysis, high energy density electrical energy storage as well as efficient drug delivery.[1] Great achievements have been made in preparation of crystalline mesoporous ceramics by traditional templating methods. Such methods generally involve infiltration of precursors within the pores of preformed inorganic or organic mesostructures, subsequent crystallization, and removal of templates.[2] For instance, Zhao *et al.* utilized mesoporous silica as a hard template to obtain mesoporous silicon carbide ceramics.[3] Wiesner *et al.* employed diblock copolymer mesophases as a soft template to fabricate multi-composition mesoporous ceramics.[4]

An interesting trend is to organize the domains of crystalline framework in an oriented way. The ordered framework can allow efficient electron or proton transportation, or exposing active facets,[5] which can greatly improve the performance in photo-voltaic conversion, catalysis or secondary battery.[6] Monocrystalline mesoporous ceramics, which are also called mesocrystals, represent a typical kind of mesoporous ceramics with oriented frameworks.[7] High-efficient solar cells, or stable lithium ion batteries have been fabricated on the basis of monocrystalline mesoporous ceramics.[8]

The main challenges in fabrication of monocrystalline mesoporous ceramics are the high cost of energy during the process, and the bad adaptability of reported methods to ceramics with complex crystal structure. The crystallization temperature of most ceramics was usually too high during solid-state thermal treatment, which of course cost too much energy. Current methods for preparation of monocrystalline mesoporous ceramics are almost limited to few ceramics such as TiO_2, SiO_2 *etc.*,[9] which have good morphology flexibility to mimic the morphology of templates under crystallization temperature. However, many of the ceramics do not have good morphology flexibility under their high crystallization temperature, thus hard to have mesocrystalline structure.

Herein, we establish a novel method which can significantly decrease the crystallization temperature of ceramics, thus the porosity and orientation of obtained ceramics are easily retained. This method is on the basis of solid-state transformation of Prussian blue analogue (PBA) mesocrystals to monocrystalline mesoporous ceramics with complex crystal structures.

As the earliest recognized coordination polymer family, Prussian blue (PB, $Fe_4[Fe(CN)_6]_3\cdot xH_2O$) and its related cyanometallate-based analogues (PBAs) have drawn much attention owing to their interesting properties, such as molecular magnetism, and catalytic activity.[10] The adjustable composition of metal ions and decomposable cyanide group make them to be good precursor for preparation of metal oxides through thermal treatment. Various nanoporous metal oxides have been fabricated through thermal decomposition of PBAs.[11] The transformation of PBAs presents an interesting solid-state chemistry concept, and can be divided into two kinds. One is single-crystalline to poly-crystalline transformation, and the other is single-crystalline to single-crystalline transformation. The single-crystalline to single-crystalline transformation is mainly based on the similar crystal structure between the precursors and the resulted metal oxides, and often could

largely reduce the energy consumption compared to traditional calcination processes. For example, Hu *et al.* reduced the synthetic temperature of hollandite type TiO_2 from 1050 °C to 600 °C.[12]

We selected $BiFeO_3$, a metal oxide with perovskite structure as the targeted material. Materials with perovskite structure, which have a cubic structure with a general formula of ABO_3, represent a famous family of functional materials. They have been widely applied in many fields such as catalysis, fuel cell, solar cell, hydrogen storage, superconducting, as well as data storage.[13] $BiFeO_3$ is a well-known material with multiple functions, such as magnetoelectric effect, photovoltaic effect, catalytic activity under irradiation of visible light.[14] The crystallization temperature of $BiFeO_3$ was generally as high as 800 °C,[15] thus it was hard to fabricate monocrystalline mesoporous $BiFeO_3$ through traditional templating method. Here, we show that monocrystalline mesoporous $BiFeO_3$ can be prepared through solid-state transformation of bismuth-containing PBA (Bi-Fe PBA) mesocrystals at a quite low temperature.

In a typical procedure, sodium citrate (SC) and polyvinyl pyrrolidone (PVP) were preferentially mixed with Bi^{3+} and $[Fe(CN)_6]^{3-}$ to control the kinetics of the crystallization. X-shape thick sheets with uniform morphology and size were formed (Fig. 1a-1). The width and thickness are of about 5 μm and 1 μm, respectively. High magnification FESEM image (inset of Fig. 1a-1) of a single sheet shows that the surface of the plate is rough. Selected area electron diffraction (SAED) patterns taken from the edge of one crystal suggest that the crystals have ordered crystallographic orientation, as shown in Fig. 1a-2. Such rough surface and single-crystal like diffraction behaviour indicate the obtained Bi-Fe PBA is mesocrystal.[7]

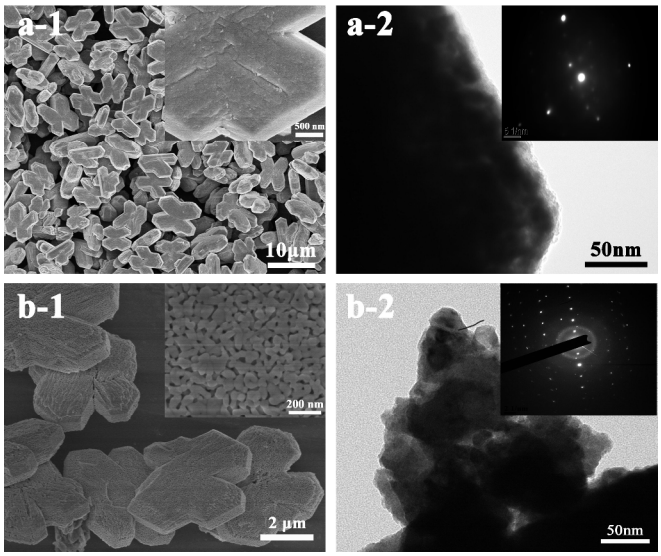

Fig. 1 (a-1) SEM image of the X-shape $Bi[Fe(CN)_6]\cdot 4H_2O$ sheets, inset shows high-magnification SEM image of the surface of a single sheet. (a-2) TEM image of the corners part of one X-shape sheet, inset shows the SAED pattern taken from the border of the sheet. (b-1) SEM image of the $BiFeO_3$ obtained by thermal conversion, inset shows FESEM image of the surface of the $BiFeO_3$. (b-2) TEM image of the thin fragment obtained from one sheet, inset shows the SAED pattern taken from the edge.

A typical XRD profile (Fig. S1) of the obtained product shows that all of the diffraction peaks can be well indexed to a pure *Cmcm* crystal structure (JCPDS file No. 84-1954).[16] And the Bi-Fe PBA was proved to be $Bi[Fe(CN)_6]\cdot 4H_2O$ *via* elemental analysis. According to the Debye-Scherrer equation, the mean grain size was calculated to be about 66 nm, demonstrating that the X-shape crystals were self-assembled from nanoparticles. In order to further confirm the composition and structure of Bi-Fe PBA, FT-IR and Mössbauer spectroscopy analysis were carried out. As shown in Fig. S2, the sharp band at 2116 cm^{-1} and a broad band at about 2054 cm^{-1} can be attributed to the stretching of C≡N groups, and the Fe-CN vibrations bands is observed at 457 cm^{-1}.[17] The broad band at 3000-3600 cm^{-1} and a band at about 1600 cm^{-1} can be assigned to the stretching and bending vibrations of the lattice water molecules, respectively.[17] In the Mössbauer spectrum (Fig. S3), only one doublet absorption peak (the isomer shift is -0.11 $mm\cdot s^{-1}$ and the quadrupole splitting is 0.69 $mm\cdot s^{-1}$) are observed, corresponding to low spin Fe^{III}, further confirming the composition of the product.[18]

The X-shape $Bi[Fe(CN)_6]\cdot 4H_2O$ crystals were converted into $BiFeO_3$ *via* calcination in air. As confirmed by XRD (Fig. S4) and Mössbauer spectrum (Fig. S5), pure-phase $BiFeO_3$ were successfully obtained at 400 °C in air. All the peaks in XRD pattern can be indexed to a rhombohedral phase with *R3c* space group (JCPDS file No. 86-1518). Two fitted magnetic (sextet) absorption spectra (the fitting parameters are showed in Table S1) are observed in the Mössbauer spectrum. The existence of two sextets is attributed to the presence of Fe^{3+} in two different crystallographic environments.[19]

$BiFeO_3$ particles well-inherited the X-shape morphology of $Bi[Fe(CN)_6]\cdot 4H_2O$, and became mesoporous as shown in Fig. 1b-1. The inset reveals that the product is porous. Nitrogen adsorption isotherm of the porous $BiFeO_3$ particles is shown in Fig. S6. The Brunauer-Emmett-Teller (BET) surface area of the products was calculated to be 24 $m^2\cdot g^{-1}$. The pore size distribution calculated by the Barrett-Joyner-Halenda (BJH) method concentrates at about 20 nm (inset graph of Fig. S6), which is in agreement with the SEM results. Periodic SAED pattern (Fig. 1b-2) taken from the fragment of an individual particle indicates the framework is monocrystalline. In conclusion, the preparation of monocrystalline mesoporous $BiFeO_3$ from thermal transformation of $Bi[Fe(CN)_6]\cdot 4H_2O$ crystals succeeded.

It is worth noting that the thermal treatment temperature at 400 °C is significantly lower than the crystallization temperature utilized in tradition preparation, for example, sol-gel method. Normally, the crystallization temperature of $BiFeO_3$ is of around 800 °C (Table S2).[15] The low temperature greatly saves the consumed energy, and is probably the reason that the walls of the mesoporous do not collapse during thermal treatment.

The solid-state transformation process was discussed to illustrate that how a monocrystalline mesoporous perovskite oxide can be formed, and to understand that why the crystallization temperature can be so low. The entire transformation process can be described as a single-crystal to single-crystal process. The single-crystal to single-crystal

process usually depends on topochemical conversion. Topochemical conversion requires strict match of crystal structures between initial and final materials, which is not the case in our work. The crystal structure of $BiFeO_3$ is different from that of $Bi[Fe(CN)_6]\cdot 4H_2O$. Therefore, oriented transformation that may take place during the thermal decomposition process has to be considered.

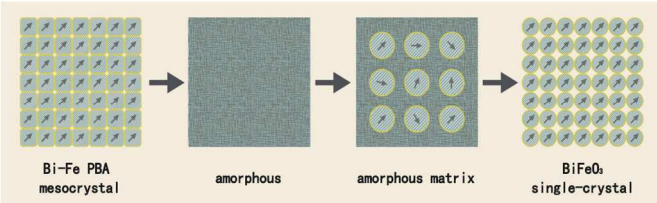

Fig. 2 Schematic illustration of the transformation process, from Bi-Fe PBA to $BiFeO_3$.

In previous reports, iron ions in PBA can be converted into amorphous oxide phase after thermal treatment.[20] Therefore, we speculated that the actual transformation process is single-crystal to amorphous at first, then to single-crystal finally. It is well-known that re-organization of domains with different orientations can happen to decrease the system energy in amorphous matrix.[21] To confirm this deduction, various samples taken at different calcination stage of Bi-Fe PBA were characterized. XRD profile confirms that amorphous phase really existed at around 300 °C stage in the calcining process as shown in Fig. S7. When the calcination temperature just reached 400 °C， partial crystalline $BiFeO_3$ phase appeared.

Such results suggest that the conversion of Bi-Fe PBA to $BiFeO_3$ is a multi-step process, as exhibited in Fig. 2. When the Bi-Fe PBA precursor undergoes heat treatment in air, they can be oxidized and transformed to amorphous matrix at first. Along with the increase of the temperature, $BiFeO_3$ can be crystallized gradually and distributed uniformly among the amorphous matrix. Then self-adjustment of the orientation of crystalline domains leads to monocrystalline framework, which is most favourable in thermal dynamic views. In general the multiple-step processes only need to overcome low energy barrier in each step, thus the crystallization temperature can be decreased.[22]

Although the calcination temperature is low, the obtained monocrystalline mesoporous $BiFeO_3$ shows good magnetic property and photocatalytic activity. Fig. 3a shows the *M-H* hysteresis loop curve. The saturated magnetization is of about 0.52 emu/g at 8k Oe, and the remanent magnetization is of about 0.035 emu/g (inset graph of Fig. 3a). Such properties are similar to the nanoparticle samples prepared at 800 °C by traditional solid-state method.[23]

As shown in Fig. 3b, almost no Rh B was removed without using catalyst, while about 97% Rh B was decomposed after 4 h in the presence of $BiFeO_3$. This result is superior to or comparable to the results in other reports,[24] which should mainly be contributed by the unique structure of the $BiFeO_3$ mesocrystals. The existence of pores could provide more active sites while the nanoscale size of the building blocks can facilitate the separation of photo-generated electrons and holes.[25] The combination of weak ferromagnetism and enhanced visible-light-induced photocatalytic activity endows the mesoporous $BiFeO_3$ promising potential for water treatment applications.

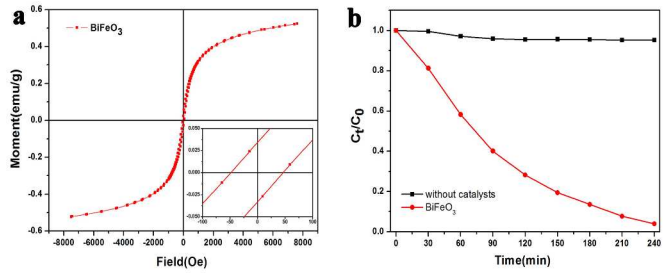

Fig. 3 (a) Magnetic hysteresis loop of $BiFeO_3$ at room temperature, inset shows the expanded view of the remanent magnetization of the sample. (b) Photocatalytic degradation efficiencies of Rh B as a function of irradiation time.

Conclusions

In conclusion, uniform $Bi[Fe(CN)_6]\cdot 4H_2O$ mesocrystalline sheets with X-shape were successfully synthesized through an additive-mediated precipitation method. By using $Bi[Fe(CN)_6]\cdot 4H_2O$ mesocrystal sheets as precursors, monocrystalline mesoporous $BiFeO_3$ was prepared at a low temperature. Due to the high crystallinity and the porous structure, the as-prepared $BiFeO_3$ showed good magnetic property and good photocatalytic activity. More interestingly, the porous structure of the monocrystalline $BiFeO_3$ ceramic may allow accommodation of guest molecules, and then to tune the magnetic property or construct multifunctional $BiFeO_3$-based magnetic composites.[26] This single-crystal to single-crystal transformation without the requirement of similar structure may open up a novel solid-state reaction way and offer great chances for the preparation of mesoporous monocrystalline materials with perovskite structure, or any other complex structure.

Acknowledgments

This work was supported by the National Natural Science Foundation of China (Grant No. 21173084) and Large Instruments Open Foundation of East China Normal University.

Notes and references

[a] *Department of Physics, Center for Functional Nanomateriels and Devices, East China Normal University, Shanghai 200241, P.R. China, Tel.: +86 021 54342940; fax: +86 21 54342940; E-mail addresses: jsjiang@phy.ecnu.edu.cn(J. S. Jiang) and mhu@phy.ecnu.edu.cn(M. Hu).*

[b] *Engineering Research Center of Advanced Glasses Manufacturing Technology, MOE, Donhua University, Shanghai 201620, PR China.*

[†] *These two authors contributed equally to this work.*

† Electronic Supplementary Information (ESI) available: XRD, FT-IR, Mössbauer spectrum of $Bi[Fe(CN)_6]\cdot 4H_2O$; XRD, Mössbauer spectrum(and Fitting Fitting parameters), Nitrogen adsorption-desorption isotherm of $BiFeO_3$; XRD of the products at different stage in calcining process; information of the crystallization temperature of $BiFeO_3$ from *Ref.* 15. See DOI: 10.1039/b000000x/

1 (a) W. Li and D. Y. Zhao, *Chem. Commun.*, 2013, **49**, 943-946; (b) S. Inagaki, S. Y. Guan, Y. Fukushima, T. Ohsuna and O. Terasaki, *J. Am. Chem. Soc.*, 1999, **121**, 9611-9614; (c) J. Liu, S. Z. Qiao, Q. H. Hu and G. Q. Lu, *small*, 2011, **7**, 425-443.

2 (a) P. D. Yang, D. Y. Zhao, D. I. Margolese, B. F. Chmelka and G. D. Stucky, *Chem. Mater.*, 1999, **11**, 2813-2826; (b) Y. Yamauchi and K. Kuroda, *Chem. Asian J.*, 2008, **3**, 66-676.

3 Y. F. Shi, Y. Meng, D. H. Chen, S. J. Cheng, P. Chen, H. F.Yang, Y. Wan and D. Y. Zhao, *Adv. Funct. Mater.*, 2006, **16**, 561-567.

4 M. Kamperman, C. B. W. Garcia, P. Du, H. Ow and U. Wiesner, *J. Am. Chem. Soc.*, 2004, **126**, 14708-14709.

5 (a) T. Kimura, H. Tamura, M. Tezuka, D. Mochizuki, T. Shigeno, T. Ohsuna and K. Kuroda, *J. Am. Chem. Soc.*, 2008, **130**, 201-209; (b) J. F. Ye, W. Liu, J. G. Cai, S. Chen, X. W. Zhao, H. H. Zhou, and L. M. Qi, *J. Am. Chem. Soc.*, 2011, **133**, 933-940; (c) Z. F. Bian, T. Tachikawa and T. Majima, *J. Phys. Chem. Lett.*, 2012, **3**, 1422-1427.

6 (a) W. H. Lin, T. F. Mark Chang, Y. H. Lu, T. Sato, M. Sone, K. H. Wei and Y. J. Hsu, *J. Phys. Chem. C*, 2013, **117**, 25596-25603; (b) J. L V. Escoto, Y. D. Chiang, K. C. W. Wu and Y. Yamauchi, *Sci. Technol. Adv. Mater.*, 2012, **13,** 013003; (c) H. X. Li, Z. F. Bian, Jian Zhu, D. Q. Zhang, G. S. Li, Y. N. Huo, H. Li and Y. F. Lu, *J. Am. Chem. Soc.*, 2007, **129**, 8406-8407.

7 (a) T. Suzuki and K. Kuroda, *J. Mater. Chem.*, 2007, **17**, 4762-4767; (b) H. Cölfen and M. Antonietti, *Angew. Chem. Int. Ed.*, 2005, **44**, 5576-5591; (c) S. H. Yu, H. Cölfen, K. Tauer and M. Antonietti, *Nat. Mater.*, 2005, **4**, 51-55.

8 (a) E. J. W. Crossland, N. Noel1, V. Sivaram, T. Leijtens, J. A. A. Webber and H. J. Snaith, *Nature*, 2013, **495**, 215-219; (b) S. Chen, M. Wang, J. F. Ye, J. G Cai, Y. R Ma, H. H Zhou and L. M. Qi, *Nano Research*, 2013, **6**, 243-252.

9 (a) Z. F. Bian, J. Zhu, F. L. Cao, Y. N. Huo, Y. F. Lu and H. X. Li, *Chem. Commun.*, 2010, **46,** 8451-8453; (b) J. Liu, B. Wang, S. B. Hartono, T. T. Liu, P. Kantharidis, A. P. J. Middelberg, G. Q. Lu, L. Z. He and S. Z. Qiao, *Biomaterials*, 2012, **33**, 970-978.

10 (a) D. M. Pajerowski, M. J. Andrus, J. E. Gardner, E. S. Knowles, M. W. Meisel and D. R. Talham, *J. Am. Chem. Soc.*, 2010, **132**, 4058-4059; (b) C. D. Wessells, R. A. Huggins and Y. Cui, *Nat. Commun.*, 2011, **2**, 550; (c) F. X. Bu, M. Hu, L. Xu, Q. Meng, G. Y. Mao, D. M. Jiang and J. S Jiang, *Chem. Commun.*, 2014, **50**, 8543-8546.

11 (a) M. Hu, A. A. Belik, M. Imura, K. Mibu, Y. Tsujimoto and Y. Yamauchi, *Chem. Mater.*, 2012, **24**, 2698-2707; (b) C. J. Du, F. X. Bu, D. M. Jiang, Q. H. Zhang and J. S. Jiang, *CrystEngComm*, 2013, **15**, 10597-10603; (c) M. Hu, J. S. Jiang and Y. Zeng, *Chem. Commun.*, 2010, **46**, 1133-1135; (d) L. Hua and Q. W. Chen, *Nanoscale*, 2014, **6**, 1236-1257.

12 M. Hu, A. A. Belik, H. Sukegawa, Y. Nemoto, M. Imura and Y. Yamauchi, *Chem. Asian J.*, 2011, **6**, 3195-3199.

13 (a) Y. Tsujimoto, K. Yamaura and E. T. Muromachi, *Appl. Sci.*, 2012, **2**, 206-219;（b）Y. Tsujimoto, C. Tasse, N. Hayashi, T. Watanabe, H. Kageyama, K. Yoshimura, M. Takano, M. Ceretti, C. Ritter and W. Paulus, *Nature*, 2007, **450**, 1062-1065; (c) M. A. Pena and J. L. G. Fierro, *Chem. Rev.*, 2001, **101**, 1981-2017.

14 (a) F. Gao, X. Y. Chen, K. B. Yin, S. Dong, Z. F. Ren, F. Yuan, T. Yu, Z. G. Zou, and J. M. Liu, *Adv. Mater.*, 2007, **19**, 2889-2892; (b) G. Catalan and J. F. Scott, *Adv. Mater.*, 2009, **21**, 2463-2485; (c) T. Choi, S. Lee, Y. J. Choi, V. Kiryukhin, S. W. Cheong, *Science*, 2009, **324**, 63-66.

15 (a) M. Valant, A. K. Axelsson and N. Alford, *Chem. Mater.*, 2007, **19**, 5431-5436; (b) M. Thrall, R. Freer, C. Martin, F. Azough, B. Patterson , R.J. Cernik, *J. Euro. Ceram. Soc.*, 2008, **28**, 2567-2572; (c) S. V. Kalinin, M. R. Suchomel, P. K. Davies and D. A. Bonnell, *J. Am. Ceram. Soc.*, 2002, **85**, 3011-3017; (d) J. Chen, X. R. Xing, A. Watson, W. Wang, R. B. Yu, J. X. Deng, L. Yan, C. Sun and X. B. Chen, *Chem. Mater.*, 2007, **19**, 3598-3600; (e) X. H. Zheng, P. J. Chen, N. Ma, Z. H. Ma and D. P. Tang, *J Mater Sci: Mater Electron*, 2012, **23**, 990-994; (f) Y. P. Wang, L. Zhou, M. F. Zhang, X. Y. Chen, J. M. Liu and Z. G. Liu, *Appl. Phys. Lett.*, 2004, **84**, 1731-1733.

16 M. Yamada and S. Yonekura, *J. Phys. Chem. C*, 2009, **113**, 21531.

17 L. F. Lin, X. J. Huang, L. S. Wang, A. Tang, *Solid State Sci.*, 2010, **12**, 1764-1769.

18 K. Maer, Jr., M. L. Beasley, R. L. Collins and W. O. Milligan, *J. Am. Ceram. Soc.*, 1968, **90**, 3201-3208.

19 T. J. Park, G. C. Papaefthymiou, A. J. Viescas, A. R. Moodenbaugh and S. S. Wong, *Nano Lett.*, 2007, **7**, 766-772.

20 (a) J. J. M. Lenders, A. Dey, P. H. H. Bomans, J. Spielmann, M. M. R. M. Hendrix, G. de With, F. C. Meldrum, S. Harder and N. A. J. M. Sommerdijk, *J. Am. Chem. Soc.*, 2012, **134**, 1367-1373; (b) R. Zboril, L. Machala, M. Mashlan and V. Sharma, *Crtst. Growth Des.*, 2004, **4**, 1317-1325.

21 (a) R. Q. Song, H. Colfen, A. W. Xu, J. Hartmann and Markus Antonietti, *Nano*, 2009, **3**,1966-1978; (b) S. Z. Deng, V. Tjoa, H. M. Fan, H. R. Tan, D. C. Sayle, M. Olivo, S. Mhaisalkar, J. Wei and C. H. Sow, *J. Am. Chem. Soc.*, 2012, **134**, 4905-4917.

22 Cölfen, H. and Antonietti, M. (2008) Nonclassical Crystallization, in Mesocrystals and Nonclassical Crystallization, John Wiley & Sons, Ltd, Chichester, UK.

23 (a) S. Li, Y. H. Lin, B. P. Zhang, Y. Wang and C. W. Nan, *J. Phys. Chem. C*, 2010, **114**, 2903-2908; (b) F. Gao, X. Y. Chen, K.B. Yin, S. Dong, Z. F. Ren, F. Yuan, T. Yu, Z. G. Zou and J. M. Liu, *Adv. Mater.*, 2007, **19**, 2889-2892.

24 (a) Y. N. Huo, M. Miao, Y. Zhang, J. Zhu and H. X. Li, *Chem. Commun.*, 2011, **47**, 2089-2091; (b) R. Q. Guo, L. Fang, W. Dong, F. G. Zheng and M. R. Shen, *J. Mater. Chem.*, 2011, **21**, 18645-18652; (c) J. Wei, C. Zhang, Z. Xu, *Mater. Res. Bulletin*, 2012, **47**, 3513-3517.

25 B. X. Li and Y. F. Wang, *J. Phys. Chem. C*, 2010, **114**, 890-896.

26 (a) C. Wang, K. E. deKrafft and W. B. Lin, *J. Am. Chem. Soc.*, 2012, **134**, 7211−7214; (b) Z. X. Wu, W. Li, P. A. Webley and D. Y. Zhao, *Adv. Mater.*, 2012, **24**, 485–491.